JOURNAL OF AIRCRAFT
Vol. 30, No. 5, Sept.–Oct. 1993

Application of Nonlinear Systems Theory to Transonic Unsteady Aerodynamic Responses

Walter A. Silva*
NASA Langley Research Center, Hampton, Virginia 23665

A methodology is presented for using the Volterra-Wiener theory of nonlinear systems in aeroservoelastic (ASE) analyses and design. The theory is applied to the development of nonlinear aerodynamic response models that can be defined in state-space form and are, therefore, appropriate for use in modern control theory. The Volterra-Wiener theory relies on the identification of nonlinear kernels that can be used to predict the response of a nonlinear system due to an arbitrary input. A numerical kernel identification technique, based on unit impulse responses, is presented and applied to a simple bilinear, single-input-single-output (SISO) system. The linear kernel (unit impulse response) and the nonlinear second-order kernel of the system are numerically identified and compared with the exact, analytically defined linear and second-order kernels. This kernel identification technique is then applied to the computational aeroelasticity program-transonic small disturbance (CAP-TSD) code for identification of the linear and second-order kernels of a NACA64A010 rectangular wing undergoing pitch at $M = 0.5$, $M = 0.85$ (transonic), and $M = 0.93$ (transonic). Results presented demonstrate the feasibility of this approach for use with nonlinear, unsteady aerodynamic responses.

Introduction

THE subject of nonlinear unsteady aerodynamics is one of great interest in the aerospace community. The interest is due to the fact that nonlinear unsteady aerodynamic behavior can have a significant effect on the performance and stability of a flight vehicle. It is important, therefore, to be able to predict and understand nonlinear unsteady aerodynamic responses.

Today's most powerful and sophisticated tools for predicting nonlinear unsteady aerodynamics are being developed in the field of computational fluid dynamics (CFD).[1] The nature and detail of the nonlinear fluid flow that is predicted by a particular flow solver depends on the governing equations that are discretized in the solver. The order of the governing flow equations can vary from the transonic small disturbance (TSD) level to the full Navier-Stokes equations. As CFD methods improve our ability to predict nonlinear unsteady flows, it is a natural and important step to investigate methods for controlling these flows in order to improve the performance and/or stability of a flight vehicle at flight conditions where nonlinear unsteady aerodynamic effects are significant.

Modern aeroservoelastic (ASE) analysis tools, such as interaction of structures, aerodynamics, and controls (ISAC)[2] and analog and digital aeroservoelastic method (ADAM)[3] are routinely used for predicting the interaction between the structural system, the aerodynamic system, and the control system of a flexible aircraft so that control laws that account for and take advantage of this flexibility can be designed. The goal of the control law design may be for flutter suppression (stability)[4] and/or for load alleviation (performance), but in either case the control system design has been limited to linear aerodynamic responses. This limitation inhibits the design and analysis of control systems that can account for flow nonlinearities such as shocks, boundary-layer effects, and separated flows. Although nonlinear aerodynamics are eventually incorporated into the control system design by way of wind-tunnel studies or semiempirical simulations, there is a very real need for modeling nonlinear aerodynamic behavior, such as that predicted by CFD codes, early in the design phase for use in ASE analysis methods. Although some work has been done in directly incorporating simple control laws into CFD codes,[5,6] these approaches do not generate a general model of the nonlinear aerodynamic responses. Instead, the control law gains have to be varied in a trial-and-error manner as flight conditions are varied. Since linear aerodynamic responses are modeled as linear systems using rational function approximations in modern ASE codes, the purpose of this research is to investigate the feasibility of modeling nonlinear aerodynamic responses as nonlinear systems, in particular, as a Volterra-Wiener nonlinear system.

The Volterra theory was developed by Volterra in 1930.[7] The theory is based on functionals, or functions of other functions, and subsequently became a generalization of the linear convolution integral approach that is applied to linear time-invariant (LTI) systems. The theory formulates the response of a nonlinear, time-invariant system as an infinite sum of multidimensional convolution integrals of increasing order, with the first term in the series being the standard linear convolution integral. Each multidimensional convolution integral in the series has an associated kernel. The first-order kernel is simply the linear unit impulse response of the system, and the higher-order kernels are measures of nonlinearity of the system response. This infinite sum of multidimensional convolution integrals is known as the Volterra Series and it is well-defined in both the time and frequency domains.

The Volterra theory has been applied primarily to nonlinear electrical and electronic systems. Wiener[8] contributed significantly to the Volterra theory and, as a result, the theory is currently referred to as the Volterra-Wiener theory of nonlinear systems. References 9 and 10 developed a kernel identification technique based on auto- and cross-correlation functions that can be applied to nonlinear, time-varying systems. The textbooks by Rugh[11] and Schetzen[12] and the work by Boyd, et al.[13] and several others[14–18] are excellent, detailed descriptions of the Volterra-Wiener theory and are highly recommended to the interested reader.

Presented as Paper 91-1110 at the AIAA/ASME/ASCE/AHS/ASC 32nd Structures, Structural Dynamics, and Materials Conference, Baltimore, MD, April 8–10, 1991; received July 29, 1991; revision received July 6, 1992; accepted for publication July 21, 1992.

*Research Engineer, Unsteady Aerodynamics Branch. Senior Member AIAA.

Application of nonlinear system theories, including the Volterra-Wiener theory, to the problem of modeling nonlinear unsteady aerodynamic responses has not been extensive. Ueda and Dowell's[19] application of the concept of describing functions to unsteady transonic aerodynamic responses is one approach. The work by Tobak and Pearson[20] involved the application of Volterra's concept of functionals to indicial aerodynamic responses for the analytical derivation and experimental determination of nonlinear stability derivatives. The work by Jenkins[21] is also an investigation into the determination of nonlinear aerodynamic indicial responses and nonlinear stability derivatives. Stalford et al.[22] successfully developed Volterra models for simulating the nonlinear behavior of a simplified nonlinear stall/poststall aircraft model and the behavior of a simplified model of wing rock.

In Ref. 22 the nonlinear aerodynamic response is analytically defined a priori so that derivation of the Volterra kernels is a straightforward procedure. In general, the nonlinear response of a given configuration at a given flight condition will not be known. The output from a CFD code provides information regarding the nonlinear aerodynamic response of the configuration at a given flight condition to a given input, but a limited amount of information can be inferred regarding the nonlinear aerodynamic response of the configuration to an arbitrary input. Prediction of the nonlinear aerodynamic response of a configuration to an arbitrary input requires identification of the nonlinear kernels of the Volterra Series for the particular configuration.

The problem of Volterra kernel identification has been addressed by Rugh,[11] Clancy and Rugh[23] for discrete systems, Schetzen,[24] and more recently Boyd et al.[25] There are several ways of identifying the Volterra kernels, both in the time and frequency domains. The methods can be applied to continuous or discrete systems,[23] such as CFD models. Recently, Tromp and Jenkins[26] applied a Laplace domain scheme and aerodynamic indicial responses for the identification of the Volterra kernels of a two-dimensional airfoil undergoing pitching motions using a Navier-Stokes flow solver. The first order, or linear, kernel was identified. The second-order kernel was identified for a sample problem, and the method of Boyd et al.[25] was suggested for identification of the second-order nonlinear kernel of the airfoil response.

An important characteristic of the Volterra-Wiener theory of nonlinear systems is that a bilinear state-space system can be realized once the nonlinear kernels of interest have been identified.[27,28] This bilinear state-space system can be used as a nonlinear aerodynamic model for aeroservoelastic analysis and design. Standard control theory techniques or the theory of bilinear optimal control can then be used for designing control systems that account for nonlinearities in the aerodynamic response.

The objective of the present research is to investigate the application of a time-domain identification technique to the three-dimensional computational aeroelasticity program-transonic small disturbance (CAP-TSD) code[29] for identification of the nonlinear, second-order kernel of a NACA64A010 rectangular wing undergoing pitch at transonic Mach numbers. This article begins with a brief description of the Volterra-Wiener theory of nonlinear systems followed by the description of a kernel identification technique based on unit impulse responses. The kernel identification technique is applied to a simple bilinear state-space system to provide insight into the application of the technique and the nature of a nonlinear kernel. The CAP-TSD code and the computational model of the rectangular wing are then described and, finally, some results for the wing are presented and discussed.

Volterra-Wiener Theory

The basic premise of the Volterra-Wiener theory of nonlinear systems is that any nonlinear system can be modeled as an infinite sum of multidimensional convolution integrals of increasing order. This infinite sum is known as the Volterra Series and it has the form

$$y(t) = \int_0^t h_1(t-\tau)u(\tau)\,d\tau + \int_0^t \int_0^t h_{2s}(t-\tau_1, t-\tau_2) \times u(\tau_1)u(\tau_2)\,d\tau_1\,d\tau_2 + \int_0^t \ldots \int_0^t h_{ns}(t-\tau_1, \ldots, t-\tau_n) \times u(\tau_1)\ldots u(\tau_n)\,d\tau_1 \ldots d\tau_n + \ldots \quad (1)$$

where $y(t)$ is the response of the nonlinear system to $u(t)$, an arbitrary input; h_1 is the first-order kernel or the linear unit impulse response; h_{2s} is the second-order kernel, and h_{ns} is the nth order kernel. It is assumed that 1) the kernels, input function, and subsequently, the output function are real-valued functions defined for

$$\tau_i \in (-\infty, +\infty), i = 1, \ldots, n, \ldots$$

2) the system is causal so that $h_{ns}(\tau_1, \ldots, \tau_n) = 0$ if any $\tau_i < 0$; and 3) the system is time invariant.

Inspection of Eq. (1) reveals some very interesting and characteristic features of the Volterra series. If the kernels of order two and above are zero, then the response of the system is linear and is completely described by the unit impulse response $h_1(t)$ and the first-order convolution integral. The assumption underlying the first-order, or linear, convolution integral is that the response of the system at a given time t is independent of the response of the system at a previous time. This is why convolution of a single unit impulse response with an arbitrary input is valid for predicting the response of a linear system. The higher order kernels h_{ns}, are the responses of the nonlinear system to multiple unit impulses, with the number of impulses applied to the system equal to the order of the kernel of interest, e.g., h_{2s} is the response of the nonlinear system to two unit impulses applied at two varying points in time, τ_1 and τ_2. The mathematical definition directly follows for the nth order kernels although visualization of these functions can become difficult for orders greater than three. The nonlinear kernels are measures of the relative influence of a previous input on the current response, which is a measure of nonlinearity. This temporal measure of nonlinearity is referred to as memory and as a result Volterra systems are sometimes referred to as nonlinear systems with memory.

The "s" in the kernel names stands for "symmetric" since $h_{2s}(\tau_1, \tau_2) = h_{2s}(\tau_2, \tau_1)$. Although, depending on the domain of integration that is chosen, the kernels can be defined in "triangular" or "regular" form, any kernel can be symmetrized without affecting the input/output relation. This is done by realizing that

$$h_{\text{sym}}(\tau_1, \ldots, \tau_n) = (1/n!)\Sigma h[\tau_{\pi(1)}, \ldots, \tau_{\pi(n)}] \quad (2)$$

where the indicated summation is over all $n!$ permutations of the integers 1 through n. For the present study, only symmetric kernels will be investigated since these are mathematically easier to interpret and intuitively easier to visualize. For the interested reader, details regarding this issue can be found in Refs. 11 and 12.

One approach for obtaining Volterra series representations of physical systems is to assume that the system is a "weakly" nonlinear system. A system that is weakly nonlinear is a system that is well-defined by the first few kernels of the Volterra series so that the magnitudes of the kernels greater than second- or third-order fall off rapidly and are negligible. Boyd et al.[25] mention some physical systems that are accurately modeled as weakly nonlinear systems, including electromechanical and electroacoustic transducers and some biological systems. In this initial study, it is assumed that the nonlinear aerodynamic system that is synthesized from the TSD potential equation is a weakly nonlinear, second-order system. Results are therefore limited to the identification of the second-order kernel, or h_{2s}.

It should also be noted that the kernels, linear and nonlinear, are input-dependent. For example, if the response of a linear system to an arbitrary input is desired, the unit impulse response of the system due to that particular type of input must first be defined. For a single-input-single-output (SISO) system, there is only one unit impulse response. For a multiple-input-multiple-output (MIMO) system, there are $n \times m$ unit impulse responses where n is the number of inputs and m is the number of outputs. These unit impulse responses are then combined to form the unit impulse matrix.

Kernel Identification

The advantage of the Volterra series approach for modeling nonlinear systems is that once the kernels are identified, the response of the nonlinear system to an arbitrary input can be predicted. The problem of kernel identification, therefore, is central to the successful generation of an accurate Volterra series representation of a nonlinear system. The most obvious approach for identifying the kernels is to derive analytical expressions for the kernels from the governing nonlinear equations of the system of interest.[30,31] Although this approach is applicable to any set of nonlinear equations, including the nonlinear fluid flow equations such as TSD, Euler, and Navier-Stokes equations, it would require some additional coding in order to numerically compute the kernels. Instead, a kernel identification technique is desired that directly uses the output of a CFD code for quick and efficient kernel identification.

Boyd et al.[25] describe a frequency-domain technique that was successfully applied to the experimental identification of the second-order kernel of a nonlinear electroacoustic transducer (speaker) system. This and other frequency-domain techniques are available, but it is preferable to use a time-domain kernel identification technique since unsteady, nonlinear CFD analyses are generally performed in the time domain. The time-domain method investigated in this study is the method of unit impulse responses.[11,12,24] Although unit impulse responses are defined for continuous systems, Clancy and Rugh[23] have shown that an equivalent technique using the unit pulse response can be used for the kernel identification of discrete nonlinear systems.

In what follows, the kernel identification technique using unit impulse responses is derived. The technique is then applied to a simple problem in order to illustrate the discrete application of the technique and the nature of the second-order kernel that is identified.

A weakly nonlinear, second-order system is described by

$$y(t) = \int_0^t h_1(t - \tau)u(\tau)\,d\tau + \int_0^t \int_0^t h_{2s}(t - \tau_1, t - \tau_2) \times u(\tau_1)u(\tau_2)\,d\tau_1\,d\tau_2 \tag{3}$$

Inputs consisting of single- and double-impulse functions can be defined as

$$u_0(t) = \delta_0(t) \tag{4}$$

$$u_1(t) = \delta_0(t) + \delta_0(t - T_1) \tag{5}$$

where T_1 is a distinct positive number. The responses of the system to these two inputs are

$$y_0(t) = h_1(t) + h_{2s}(t, t) \tag{6}$$

$$y_1(t) = h_1(t) + h_1(t - T_1) + h_{2s}(t, t) + 2h_{2s}(t, t - T_1) + h_{2s}(t - T_1, t - T_1) \tag{7}$$

Solving for the second-order kernel

$$h_{2s}(t, t - T_1) = \tfrac{1}{2}[y_1(t) - y_0(t) - y_0(t - T_1)] \tag{8}$$

which is the value of the second-order kernel for any value of T_1.

The procedure for computing h_{2s} is as follows. First, $y_0(t)$, which is the response of the system to a unit impulse response applied at t, is generated. Then, since the system is time invariant, y_0 is shifted to a new $t - T_1$, which becomes $y_0(t - T_1)$. The response of the system to two unit impulses, one at t and one at $t - T_1$, or $y_1(t)$, is generated and finally all three responses are substituted into Eq. (8). The second-order kernel, h_{2s} is a two-dimensional function of time. That is, it is a function of t and a function of time lag T_1 so that for every value of T_1 that is used, a new function of t is defined. These sets of functions of time are referred to as "terms" of the kernel. The first term of h_{2s} is defined when $T_1 = 0$, or when both unit impulse inputs are applied at the same point in time. When $T_1 = 0$, Eq. (8) reduces to

$$\begin{aligned} h_{2s}(t, t) &= \tfrac{1}{2}[y_1(t) - y_0(t) - y_0(t)] \\ &= \tfrac{1}{2}y_1(t) - y_0(t) \end{aligned} \tag{9}$$

The second term of the kernel depends on the next value of T_1 selected. The number of T_1, or the number of terms needed to accurately define a second-order kernel depends on the nonlinear system under investigation.

In addition, the linear portion of the nonlinear response can be identified when $T_1 = 0$. It is important to realize that the linear portion of the nonlinear response is not, in general, equivalent to the purely linear response. For example, for an aerodynamic system, the linear response computed using the linear equations (flat plate) is not identical to the linear portion of the response computed using the nonlinear equations (thickness).

The linear portion of the nonlinear response is defined as follows. The response of the system represented by Eq. (3) to $2u_0(t)$ is

$$y_2(t) = 2h_1(t) + 4h_{2s}(t, t) \tag{10}$$

Then, solving simultaneously with $y_0(t)$ results in

$$h_1(t) = 2y_0(t) - \tfrac{1}{2}y_2(t) \tag{11}$$

which is the unit impulse response of the linear portion of the nonlinear response.

The equations derived above for h_{2s} are clear and simple measures of nonlinearity. In these equations, nonlinearity is measured as a deviation from linear behavior. This is evident in that h_{2s} is identically zero for a linear system due to the principle of linear superposition. Therefore, an additional benefit of the second-order kernel is that it can be used to measure the true linearity of a system that is classified as being linear, or for establishing boundaries beyond which the assumptions of linearity begin to fail. Definitions of higher-order kernels can be derived in the same way as for h_{2s}, by applying the appropriate number of unit impulses to the system.

Once h_{2s} is identified, the response of the weakly nonlinear, second-order system to an arbitrary input can be determined. A further advantage of the Volterra theory of nonlinear systems is that a bilinear state-space system can be realized once the kernels are identified, generating a nonlinear aerodynamic state-space system that is amenable for use with modern control theory. The relationship between the Volterra kernels and the bilinear state-space formulation is as follows.

It is well known that for a linear system described by the following state-space representation

$$\begin{aligned} \dot{x} &= Ax + Bu \\ y &= Cx \end{aligned} \tag{12}$$

(where the D matrix, or feedthrough term, has been set to zero) the system's unit impulse response is given by

$$h(t) = C[\exp(At)]B \tag{13}$$

If the unit impulse response of a linear system is known, then a state-space realization can be obtained using standard linear system realization techniques. In a natural extension to this concept, a Volterra system can be modeled by a bilinear state-space system as follows:

$$\begin{aligned} \dot{x} &= Ax + Nxu + Bu \\ y &= Cx \end{aligned} \tag{14}$$

where the matrix N is a measure of the nonlinearity of the system. The system is linear when $N = 0$, as it is reduced to Eq. (12). The relationship between the second-order Volterra kernel and the bilinear state-space formulation is

$$h_{2\text{reg}}(t_1, t_2) = C[\exp(At_1)]N[\exp(At_2)]B \tag{15}$$

where the subscript "reg" stands for the "regular" definition of the kernel. Equation (2) can then be used to compute the symmetric kernel h_{2s} from $h_{2\text{reg}}$.

Example Problem

Assume a system described by the following differential equation:

$$\ddot{y}(t) + a_1\dot{y}(t) + a_0y(t) = b_0u(t) + n_0y(t)u(t) \tag{16}$$

In bilinear state-space form, Eq. (16) can be rewritten as Eq. (14) where

$$A = \begin{bmatrix} 0 & 1 \\ -a_0 & -a_1 \end{bmatrix}, \quad N = \begin{bmatrix} 0 & 0 \\ n_0 & 0 \end{bmatrix}, \quad B = \begin{bmatrix} 0 \\ b_0 \end{bmatrix}$$

$$C = [1 \quad 0]$$

Values for the A, N, and B matrices were arbitrarily chosen as $a_0 = 2$, $a_1 = 3$, $n_0 = -6$, and $b_0 = 1$. The linear response of this system is obtained by setting $n_0 = 0$. An arbitrary input, shown in the inset of Fig. 1, was defined as

$$\begin{aligned} u_{\text{arb}}(t) &= 0.0, \quad t < 0.1 \quad \text{and} \quad t > 1.1 \\ &= t - 0.1, \quad 0.1 \le t \le 1.1 \end{aligned}$$

and applied to discretized versions of the linear ($N = 0$) and nonlinear (bilinear) systems in order to examine the differences in the responses due to this arbitrary input using a time step of 0.01. The responses can be seen in Fig. 1 where it is clear that the effect of the added nonlinearity is to reduce the level of the linear response.

Application of the kernel identification technique to continuous systems requires the use of unit impulse inputs. The equivalent of a unit impulse input for discrete systems is a unit pulse input defined as

$$\begin{aligned} u_p(t) &= 1, \qquad t = t0 \\ &= 0, \qquad t \ne t0 \end{aligned}$$

where $t0$ can be any time step since the system is time invariant. Also, the unit impulse response of a continuous system is approximately equal to the unit pulse response of the discretized version of the same system divided by the time step used in the discretization. The discrete responses are therefore divided by the time step so that comparisons with the continuous, or analytical, responses can be made.

The unit pulse input $u_p(t)$ was applied to the discretized linear system and the resultant unit pulse response was compared to the analytical (or continuous) unit impulse response of the system from Eq. (13). This comparison is presented in Fig. 2, showing excellent agreement. The slight difference between the two responses is a result of the time step ($DT = 0.01$) that was used. A smaller time step improves the accuracy of the unit pulse response.

The unit pulse input was then modified to include two unit pulses for identification of the second-order kernel so that

$$\begin{aligned} u_p(t) &= 1, \quad t = t0 \quad \text{and} \quad t = t1 \\ &= 0, \quad t \ne t0 \quad \text{and} \quad t \ne t1 \end{aligned}$$

where the value of $t1$ is a time step such that $t1 - t0 = T_1$. The $t0$ was held fixed while the $t1$ was varied in order to vary T_1. The value of T_1 was varied in increments of 10 time steps, or 0.1 s. The first term of the second-order kernel corresponds to $T_1 = 0.0$; the second term of the second-order kernel corresponds to $T_1 = 10$ time steps; the third term corresponds to $T_1 = 20$ time steps. A total of 20 terms were generated and the resulting second-order kernel is shown in Fig. 3 as a function of t and T_1. In Fig. 3, TB is the second term of the kernel ($T_1 = 10$ time steps), TC is the third term, TD is the fourth term, and the first term, TA, is not visible because it was zero. As can be seen, the second-order kernel is a two-dimensional function that varies smoothly with t and T_1. It can also be seen that the second-order nonlinear response of the system at each T_1 exhibits a rapid initial growth, reaches

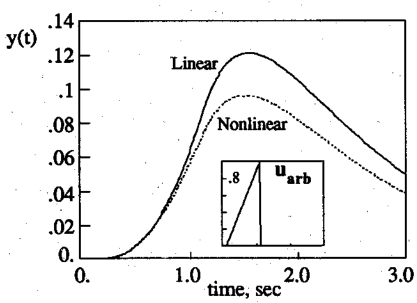

Fig. 1 Response of the linear system ($N = 0$) and the nonlinear (bilinear) system due to the input shown in the inset for the example problem.

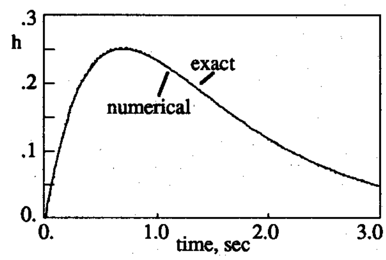

Fig. 2 Comparison of the analytical and numerically identified linear unit impulse responses for the example problem.

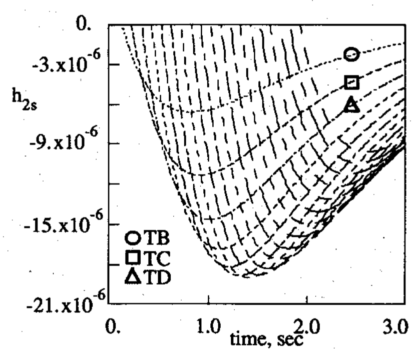

Fig. 3 Numerically identified second-order kernel at 20 values of time lag for the example problem.

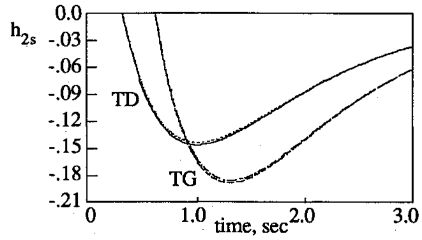

Fig. 4 Comparison of analytical and numerically identified second-order kernels at two values of time lag for the example problem.

a maximum response, and then begins to dissipate. The fact that the second-order kernel is negative is consistent with the result in Fig. 1 where it was shown that the added nonlinear terms reduced the response of the system from the purely linear response. Inspection of a nonlinear kernel, therefore, can provide a significant amount of information regarding the behavior of a nonlinear system in terms of amplitude and time lag variations. This is important information for the design of effective control systems.

The exact, analytical second-order kernel of the bilinear system was computed using Eq. (15). The analytical second-order kernel is not a symmetric kernel and so it must be symmetrized before it can be compared with the numerically identified symmetric second-order kernel. Symmetrization of the analytical kernel is performed by using Eq. (2). The numerically identified, or discrete, kernel is divided by the square of the time step so that it can be compared with the analytical, or continuous, kernel. The symmetrized analytical second-order kernel and the symmetric, numerically identified second-order kernel are shown in Fig. 4 for two time lags, TD (30 time steps) and TG (60 time steps). The comparison is excellent with slight differences occurring around the regions of maximum response. Again, improved accuracy can be achieved by using a smaller time step in the numerical identification technique. The important point to be made here, however, is that the use of discrete, unit pulses can be used to identify the discrete, second-order Volterra kernel of a discrete nonlinear system.

Computational Procedures

The CAP-TSD program is a finite-difference program which solves the general-frequency modified TSD potential equation. Details regarding the algorithm and code can be found in Refs. 32–36.

The CAP-TSD program can treat configurations with combinations of lifting surfaces and bodies including canard, wing, tail, control surfaces, tip launchers, pylons, fuselage, stores, and nacelles. The code was recently applied to the active flexible wing (AFW) wind-tunnel model, which included modeling of the fuselage and tip stores, for prediction of the model's transonic aeroelastic behavior.[36]

The code has an exponential pulse capability that can be used for generating unsteady aerodynamic pitch, plunge, and modal responses. The pulse and pulse rate are defined as

$$p(t) = \delta_0 \exp[-w(t - tc)^2] \tag{17}$$

$$\dot{p}(t) = -2w(t - tc)p(t) \tag{18}$$

where t and tc are in terms of nondimensional time steps. For pitching motions, the angle-of-attack input function is defined using Eq. (17), and the rate of change of angle of attack, or angle-of-attack rate is defined using Eq. (18). These functions of time then become part of the downwash equation which, for simple pitching motions is

$$f(x, t)^{\pm} = \frac{dz^{\pm}}{dx} - \alpha(t) - \dot{\alpha}(t)(x - x_{\text{pitch}})/U_{\infty} \tag{19}$$

where the plus and minus signs indicate upper and lower surfaces of the airfoil. The first term in Eq. (19) is the airfoil geometry slopes, followed by the angle of attack, and by the angle-of-attack rate multiplied by the pitch distance where x_{pitch} is the pitch axis. The downwash provides the boundary condition defined at the $z = 0$ plane required to complete the solution of the TSD equations. For the linear aerodynamic solution, or flat plate solution, the airfoil geometry slopes are zero and the downwash becomes a function of angle of attack and angle-of-attack rate only.

The computational grid of the NACA64A010 rectangular wing is dimensioned 137 by 40 by 84 grid points in the x, y, and z directions, respectively. The wing has an aspect ratio of 3, but the computational domain covers only one semispan due to flow symmetry.

Results and Discussion

Before the kernel identification technique was applied to an aerodynamic system, the appropriate excitation input had to be defined. It was obvious that the excitation input had to be a perturbation of the downwash, Eq. (19). The excitation input could, therefore, be composed of one or a combination of the parameters that define the downwash. In addition, the excitation input had to be of an "impulsive" nature so that the theoretical assumptions used in the derivation of the kernel identification technique were maintained.

The requirement that the excitation input be impulsive disallowed the use of the exponential pulse capability defined in the CAP-TSD code, Eqs. (17) and (18). The aerodynamic response induced by an exponential pulse input is a response of the aerodynamic system to a smoothly varying function of angle of attack and a smoothly varying function of angle-of-attack rate. This response cannot be referred to as the unit pulse response of the system, and therefore, cannot be used in the linear convolution integral to predict the linear response of the system or in the identification of the nonlinear kernels. The correct excitation input should, therefore, be of a unit magnitude and should be applied at only one time step, as was earlier presented for the example problem.

Based on this reasoning, the unit pulse inputs available are then

$$\begin{aligned} \alpha(t) &= 0.01745 \text{ rad}(=1 \text{ deg}), \qquad t = t0 \\ &= 0.0, \qquad t \neq t0 \end{aligned}$$

with $\dot{\alpha}(t) = 0.0$ everywhere, or

$$\begin{aligned} \dot{\alpha}(t) &= 1 \text{ rad/s}, \qquad t = t0 \\ &= 0.0, \qquad t \neq t0 \end{aligned}$$

with $\alpha(t) = 0.0$ everywhere, or a combination of both angle of attack and angle-of-attack rate inputs. Also, due to the impulsive nature of the unit pulse inputs, a very small time step of DT = 0.0001 had to be used in order to obtain smooth aerodynamic responses. All dynamic responses, linear and nonlinear, were 500 time steps in length. It should be noted that this choice of time step and number of time steps results in only 0.05 chords of travel. This very small time sample is dominated by the high-frequency content of the response, and so the results that follow are limited to high-frequency responses.

The application of the unit angle-of-attack pulse input resulted in very small aerodynamic responses for both the linear (flat plate) and the nonlinear (thickness) aerodynamic solutions using CAP-TSD. An attempt to identify the nonlinear kernel using these responses resulted in numerical noise and was not possible. The second type of input, the unit angle-of-attack rate pulse input, provided sufficient excitation of the nonlinear equations so that a nonlinear kernel could be identified, as will be seen. The combined unit angle-of-attack and unit angle-of-attack rate inputs resulted in responses that were only marginally different from the unit angle-of-attack rate responses. As a result of these preliminary investigations, all subsequent analyses are based on unit angle-of-attack rate pulse inputs only. Also, only lift coefficient responses to pitching motions about the quarter-chord location are investigated in this study, although the techniques presented are applicable to any force coefficient response including generalized aerodynamic forces.

For the results that follow, P1 is the unit pulse response at $t0$; P2 is the unit pulse response at $t = t0 + T_1$; P12 is the response due to a unit pulse at $t = t0$ and another unit pulse at $t = t0 + T_1$; and P11 is the response due to two unit pulses at time $t = t0$. The unit angle-of-attack rate inputs were applied at the 60th, 110th, and 160th time steps which translates to time lags equal to 0, 50, and 100 time steps. The choice of these time steps was arbitrary and the choice of the 60th time step as the first response, or as the P1 response, was done in order to avoid any numerical transients that might occur when the nonlinear aerodynamic analyses are initiated from steady-state solutions.

Linear Kernel Identification

The P1 linear (flat plate) lift-coefficient response shown in Fig. 5 has the characteristics that are typical of a unit pulse response. That is, the initial part of the response is impulsive and the latter part of the response is a damped transient. It should be restated that the time step at which the input is applied is not important since the linear system is time invariant.

The linear convolution integral

$$y(t) = \int_0^t h(t - \tau)u(\tau)\, d\tau \tag{20}$$

was used to verify that P1 (Fig. 5) was indeed a unit pulse response. This was done by first generating a linear (flat plate) lift-coefficient response to an arbitrary input using the CAP-TSD exponential pulse capability, Eqs. (17) and (18) at $M = 0.85$. The pulse was defined with a $w = 90{,}000$, $\delta_0 = 0.009$ rads (0.5 deg), and centered at $tc = 250$ time steps. The response to this exponential pulse, which will be refered to as the linear arbitrary response, is shown in Fig. 6 along with the angle of attack (inset) and the corresponding angle-of-attack rate functions generated by Eqs. (17) and (18). It should be restated that this response is of a relatively high frequency which, as can be seen in Fig. 6, is influenced primarily by the angle-of-attack rate input.

The linear convolution integral was then evaluated using the angle-of-attack rate function, presented in Fig. 6, as the input u, and the P1 response shown in Fig. 5 as the unit impulse response h. A comparison of the linear arbitrary response shown in Fig. 6 and the response computed from the linear convolution of P1 and the angle-of-attack rate function is presented in Fig. 7. The excellent agreement between the two responses verifies the use of the unit angle-of-attack rate pulse input for generating unit pulse responses that can be used for predicting high-frequency arbitrary responses. However, accurate prediction of low-frequency responses, where the angle of attack input becomes significant, needs further development.

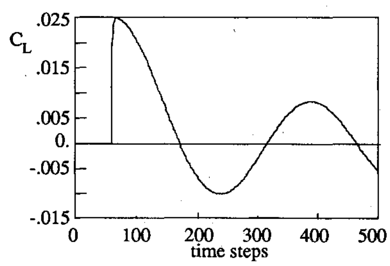

Fig. 5 Lift-coefficient unit pulse response due to pitch at the quarter-chord location for the linear (flat plate) aerodynamic solution at $M = 0.85$.

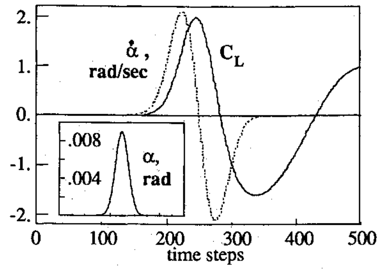

Fig. 6 Lift-coefficient response to the pitching motion about the quarter-chord location described by the angle of attack (inset) and angle-of-attack rate functions for the linear aerodynamic (flat plate) solution at $M = 0.85$.

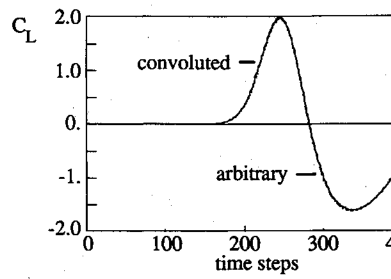

Fig. 7 Comparison of lift-coefficient responses due to the exponential pitch pulse shown in Fig. 6, for the CAP-TSD solution, the convolution of P1 (Fig. 5) and the angle-of-attack rate (Fig. 6).

Nonlinear Kernel Identification

The nonlinear aerodynamic responses were computed about steady-state converged solutions of the NACA64A010 rectangular wing at 0-deg angle of attack. These steady-state solutions consisted of about 2500–5000 time steps using a time step DT = 0.01. The gas medium used in the nonlinear analyses was air which corresponds to a $\gamma = 1.4$. The assumption of time invariance was verified for the nonlinear aerodynamic responses.

At $M = 0.85$, in the steady solution, a strong shock is present at the 60% chord location so that a level of nonlinear response should be noticed when identification of the second-order kernel is performed. The nonlinear P1, P2, P12, and P11 responses of the NACA64A010 wing at $M = 0.85$ are shown in Fig. 8. The linear portion of the nonlinear response, or h_1 [Eq. (6)], is computed first as

$$h_1 = 2(\text{P1}) - 0.5(\text{P11})$$

The linear unit pulse response from the linear (flat plate) solution is "h" and should not be confused with "h_1." Figure 9 is a comparison of these two unit pulse responses where the difference is small but noticeable, in terms of an associated time lag for the h_1.

The first term of the second-order kernel was computed using

$$\text{H2S1} = 0.5(\text{P11} - \text{P1} - \text{P1}) = 0.5(\text{P11}) - \text{P1}$$

which corresponds to $T1 = 0.0$. The nonlinear P2A and P12A responses were computed using $T_1 = 50.0$ and the nonlinear P2B and P12B responses were computed using $T_1 = 100.0$. The P2A, P12A, P2B, and P12B responses were used for computing the second and third terms of the second-order kernel, respectively, as

$$\text{H2S2} = 0.5(\text{P12A} - \text{P2A} - \text{P1})$$

$$\text{H2S3} = 0.5(\text{P12B} - \text{P2B} - \text{P1})$$

Notice that computation of additional terms of the second-order kernel requires only the generation of the appropriate

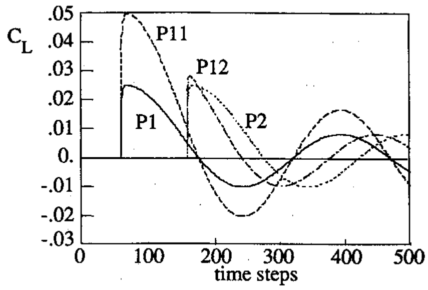

Fig. 8 Nonlinear (thickness) lift-coefficient unit pulse responses P1, P2, P11, and P12 due to pitch at the quarter-chord location for the NACA64A010 rectangular wing at $M = 0.85$ and $\gamma = 1.4$.

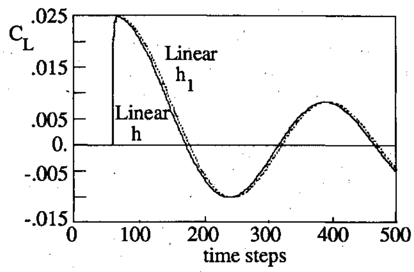

Fig. 9 Comparison of the lift-coefficient responses due to pitch at the quarter-chord location for the linear (flat plate) case and the linear portion of the nonlinear (thickness) response case at $M = 0.85$ and $\gamma = 1.4$.

P12 response since the P1 response needs to be computed only once, and the P2 response is just the P1 response shifted in time.

The three terms of the $M = 0.85$ second-order kernel, H2S1, H2S2, and H2S3, are shown in Fig. 10. It can be seen that the identified second-order kernel, although noisy at the smaller magnitudes, does exhibit a particular shape which is not numerical noise. The small values of the $M = 0.85$ second-order kernel are indications that the nonlinearities at this condition are small. This is also consistent with the result presented for the example problem where the second-order kernel identified for that case was on the order of 1.e-06. Also, the approach to zero values of the second-order kernel as time lag is increased, or as more terms are computed, is as expected since the second-order kernel is a finite and bounded function of time. The $M = 0.85$ second-order kernel therefore exhibits behavior that is characteristic of a second-order kernel.

The same three terms of the second-order kernels at $M = 0.5$ and $M = 0.93$ were also identified. At $M = 0.93$, the shock was located at the trailing edge. Figure 11 is a comparison of the nonlinear unit pulse responses of the NACA-64A010 rectangular wing at $M = 0.5$, 0.85, and 0.93. It is noticed that the amplitude and frequency of these unit pulse responses decreases as Mach number is increased. This, of course, is configuration- and motion-dependent so that, e.g., for a plunging motion, this same trend may not occur. Comparison of the second-order kernels for all three Mach numbers reveals a surprising and interesting result. Figure 12 presents the three terms of the $M = 0.5$ second-order kernel and Fig. 13 presents the three terms of the $M = 0.93$ second-order kernel. At first glance, and comparing with the three terms of the $M = 0.85$ second-order kernel (Fig. 10), it appears that the magnitude of the second-order kernels decreases with increasing Mach number. This is the reverse trend that is expected since the second-order kernel should increase with increasing levels of nonlinearity, or in this case, with an increase in Mach number.

However, this preliminary comparison is not complete. An appropriate comparison of the second-order kernels of the three Mach numbers should account for the differences in the magnitude of the unit pulse responses at each Mach number.

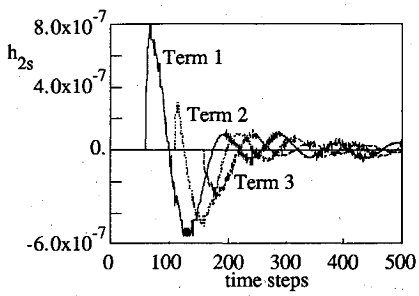

Fig. 10 Three terms of the second-order kernel of lift coefficient due to pitch about the quarter-chord location for the NACA64A010 rectangular wing at $M = 0.85$ and $\gamma = 1.4$.

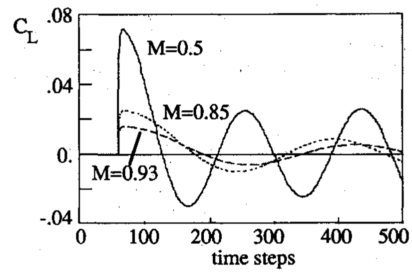

Fig. 11 Comparison of nonlinear (thickness) lift-coefficient unit pulse responses due to pitch at the quarter-chord location for $M = 0.5$, $M = 0.85$, and $M = 0.93$ with $\gamma = 1.4$.

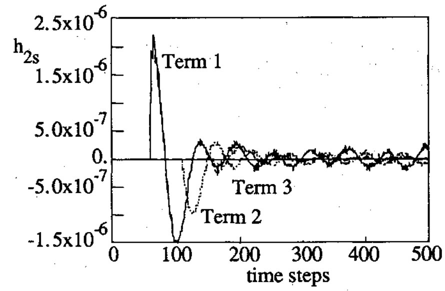

Fig. 12 Three terms of the second-order kernel of lift coefficient due to pitch about the quarter-chord location for the NACA64A010 rectangular wing at $M = 0.50$ and $\gamma = 1.4$.

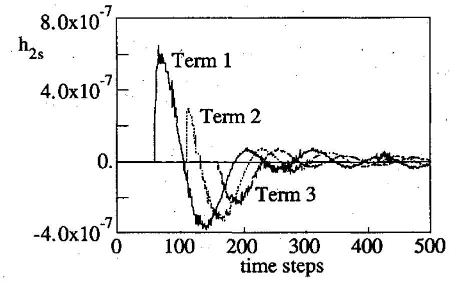

Fig. 13 Three terms of the second-order kernel of lift coefficient due to pitch about the quarter-chord location for the NACA64A010 rectangular wing at $M = 0.93$ and $\gamma = 1.4$.

If the maximum absolute value of each of the three terms of the second-order kernels is divided by the maximum value of the unit pulse response of each corresponding Mach number, the resulting values would be better indicators of the relative magnitude of the nonlinear effects. A bar chart of these values, referred to as the relative nonlinearity, for the three Mach numbers is presented in Fig. 14 for all three terms of the second-order kernels. Figure 14 does indeed show the growth of relative nonlinearity as Mach number is increased for all three terms of the second-order kernels and, in particular, the sudden increase in the first term at $M = 0.93$.

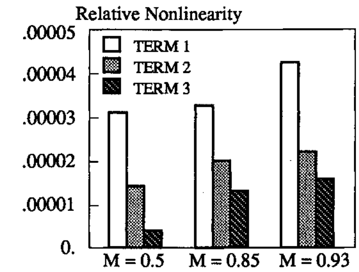

Fig. 14 Relative nonlinearity for each of the three terms of the second-order kernel at $M = 0.5$, $M = 0.85$, and $M = 0.93$.

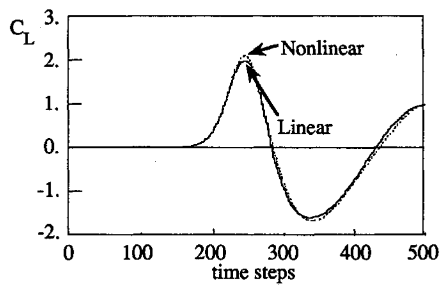

Fig. 15 Comparison of linear (flat plate) and nonlinear (thickness) lift-coefficient responses due to the exponential pitch pulse shown in Fig. 6 at $M = 0.85$ and $\gamma = 1.4$ (for nonlinear case).

A qualitative interpretation of the second-order kernels identified at $M = 0.5$, $M = 0.85$, and $M = 0.93$ would imply that a nonlinear response at these Mach numbers is dominated by an in-phase increase in magnitude (the first term) and subsequent, but smaller, time-lagged variations in the response. This is, in fact, a reasonable interpretation as can be seen in Fig. 15, which is a comparison of the linear (flat plate) aerodynamic and nonlinear (thickness) aerodynamic responses at $M = 0.85$ due to the same exponential pulse function described in Fig. 6. The nonlinear response is larger in magnitude at the regions of maximum response and exhibits some phase difference with respect to the linear response.

The results presented thus far are encouraging and support the feasibility and applicability of the Volterra series approach for the modeling of nonlinear unsteady aerodynamic responses. Additional work is needed for determining the minimum number of terms of the second-order kernel that are required for accurate prediction of responses to arbitrary inputs, in applying the unit pulse response technique to lower frequency responses where the effect of angle of attack inputs will be more significant, and in evaluating the third-order kernels for verification of the assumption of a weakly nonlinear system.

Conclusions

The Volterra-Wiener theory of nonlinear systems was briefly described and presented as a method for modeling nonlinear aerodynamic responses for use in ASE analysis and design. Successful application of the theory is contingent upon the successful identification of the nonlinear kernels. Although several methods for identifying the kernels exist, the method investigated in this study was a time-domain technique, based on unit impulse responses. The technique was described and applied to a simple bilinear (nonlinear) system for illustrative purposes and to verify the application of the technique to discrete nonlinear systems. The first order, or linear, kernel and the second-order nonlinear kernel of the simple system were accurately identified using the technique. Interpretations of the second-order kernel were also presented.

The kernel identification technique was then applied to a NACA64A010 rectangular wing using the CAP-TSD code. Application of the kernel identification technique to the aerodynamic model began with the identification of the first-order kernel due to the linear aerodynamic response (flat plate solution) of the wing in pitch about the quarter-chord location. It was shown that a unit impulse response, or, for discrete systems, a unit pulse response, can be accurately computed by a unit excitation of rate of angle of attack in the downwash function for predicting linear high-frequency responses. Additional work needs to be performed for prediction of low-frequency responses.

Identification of the second-order kernel due to pitching motions about the quarter-chord location was then performed using the same unit angle-of-attack rate pulse input that was used for identification of the linear kernel. Nonlinear (transonic) aerodynamic unit pulse responses were computed at $M = 0.5$, 0.85, and 0.93 where strong shocks are present at the $M = 0.85$ and the $M = 0.93$ conditions. Three terms of the second-order kernels for the three Mach numbers were then identified and discussed. The results are encouraging, although additional effort is required for determining the number of terms of the second-order kernel that are required for accurate prediction of nonlinear responses to arbitrary inputs, and in verifying that the assumption of a weakly nonlinear second-order system is accurate for transonic aerodynamic responses.

References

[1]Edwards, J. W., and Thomas, J. L., "Computational Methods for Unsteady Transonic Flows," *Unsteady Transonic Aerodynamics*, edited by D. Nixon, Vol. 120, Progress in Astronautics and Aeronautics, AIAA, Washington, DC, 1989, Chap. 5, pp. 211–261.

[2]Peele, E. L., and Adams, W. M., Jr., "A Digital Program for Calculating the Interaction Between Flexible Structures, Unsteady Aerodynamics, and Active Controls," NASA TM-800040, Jan. 1979.

[3]Noll, T. E., Blair, M., and Cerra, J., "An Aeroservoelastic Analysis Method for Analog or Digital Systems," *Journal of Aircraft*, Vol. 23, No. 11, 1986, pp. 852–858.

[4]Perry, B., III, Mukhopadhyay, V., Hoadley, S. T., Cole, S. R., Buttrill, C. S., and Houck, J. A., "Design, Implementation, Simulation, and Testing of Digital Flutter Suppression Systems for the Active Flexible Wing Wind-Tunnel Model," Seventeenth International Council of the Aeronautical Sciences, ICAS Paper 90-1.3.2, Stockholm, Sweden, Sept. 9–14, 1990.

[5]Ide, H., and Ominsky, D., "Simulation of Static and Dynamic Aeroelastic Behavior of a Flexible Wing with Multiple Control Surfaces," Thirty-first Structures, Structural Dynamics, and Materials Conf., AIAA Paper 90-1075, Long Beach, CA, April 2–4, 1990.

[6]Lee, E. M., and Batina, J. T., "Conical Euler Simulation and Active Suppression of Delta Wing Rocking Motion," NASA TM-102683, Oct. 1990.

[7]Volterra, V., *Theory of Functionals and of Integral and Integro-Differential Equations*, Dover, New York, 1959.

[8]Wiener, N., "Response of a Nonlinear Device to Noise," Radiation Lab., Massachusetts Inst. of Technology, Rept. 129, Cambridge, MA, April 1942; also published as U.S. Dept. of Commerce Publications PB-58087.

[9]Lee, Y. W., and Schetzen, M., "Measurement of the Wiener Kernels of a Non-Linear System by Cross Correlation," *International Journal of Control*, Vol. 2(3), Sept. 1965, pp. 237–254.

[10]Ku, Y. H., and Su, C. C., "Volterra Functional Analysis of Nonlinear Time-Varying Systems," *Journal of the Franklin Institute*, Vol. 284, No. 6, 1967, pp. 344–365.

[11]Rugh, W. J., *Nonlinear System Theory, The Volterra-Wiener Approach*, Johns Hopkins Univ. Press, Baltimore, MD, 1981.

[12]Schetzen, M., *The Volterra and Wiener Theories of Nonlinear Systems*, Wiley, New York, 1980.

[13]Boyd, S., Chua, L. O., and Desoer, C. A., "Analytical Foundations of Volterra Series," *IMA Journal of Mathematical Control and Information*, Vol. 1, 1984, pp. 243–282.

[14]Brilliant, M. B., "Theory of the Analysis of Nonlinear Systems," TR 345, Massachusetts Inst. of Technology Research Lab. of Electronics, Cambridge, MA, March 1958.

[15]Boyd, S. P., "Volterra Series: Engineering Fundamentals," Ph.D. Dissertation, Univ. of California, Berkeley, CA, 1985.

[16]Boyd, S. P., and Chua, L. O., "Fading Memory and the Problem of Approximating Nonlinear Operators with Volterra Series," *IEEE Transactions on Circuits and Systems*, Vol. CAS-32, No. 11, 1985, pp. 1150–1161.

[17]Ku, Y. H., and Wolf, A. A., "Volterra-Wiener Functionals for the Analysis of Nonlinear Systems," *Journal of the Franklin Institute*, Vol. 281, No. 1, 1966, pp. 9–26.

[18]Bedrosian, E., and Rice, S. O., "The Output Properties of Volterra Systems (Nonlinear Systems with Memory) Driven by Harmonic and Gaussian Inputs," *Proceedings of the IEEE*, Vol. 59, No. 12, 1971, pp. 1688–1707.

[19]Ueda, T., and Dowell, E. H., "Flutter Analysis Using Nonlinear Aerodynamic Forces," AIAA/ASME/ASCE/AHS 23rd Structures, Structural Dynamics, and Materials Conf., New Orleans, LA, May 10–12, 1982.

[20]Tobak, M., and Pearson, W. E., "A Study of Nonlinear Longitudinal Dynamic Stability," NASA TR R-209, Sept. 1964.

[21]Jenkins, J. E., "Relationships Among Nonlinear Aerodynamic Indicial Response Models, Oscillatory Motion Data, and Stability Derivatives," AIAA Atmospheric Flight Mechanics Conf., AIAA Paper 89-3351, Boston, MA, Aug. 14–16, 1989, pp. 43–51.

[22]Stalford, H., Baumann, W. T., Garrett, F. E., and Herdman, T. L., "Accurate Modeling of Nonlinear Systems Using Volterra Series Submodels," 1987 American Control Conf., American Automatic Control Council 87CH2378-8, Minneapolis, MN, June 10–12, 1987, pp. 886–891.

[23]Clancy, S. J., and Rugh, W. J., "A Note on the Identification of Discrete-Time Polynomial Systems," *IEEE Transactions on Automatic Control*, Vol. AC-24, No. 6, 1979.

[24]Schetzen, M., "Measurement of the Kernels of a Nonlinear System of Finite Order," *International Journal of Control*, Vol. 1(3), March 1965, pp. 251–263; see also Corrigendum, Vol. 2(4), Oct. 1965, p. 408, pp. 975–978.

[25]Boyd, S., Tang, Y. S., and Chua, L. A., "Measuring Volterra Kernels," *IEEE Transactions on Circuits and Systems*, Vol. CAS-30, No. 8, 1983.

[26]Tromp, J. C., and Jenkins, J. E., "A Volterra Kernel Identification Scheme Applied to Aerodynamic Reactions," AIAA Atmospheric Flight Mechanics Conf., AIAA Paper 90-2803, Portland, OR, Aug. 20–22, 1990.

[27]Clancy, S. J., and Rugh, W. J., "On the Realization Problem for Stationary, Homogenous, Discrete-Time Systems," *Automatica*, Vol. 14, 1978, pp. 357–366.

[28]King, A. M., and Skelton, R. E., "Model Reduction for Discrete Bilinear Systems," *IEEE Transactions on Automatic Control*, Vol. AC-24, No. 6, 1979, pp. 345–354.

[29]Batina, J. T., "Efficient Algorithm for Solution of the Unsteady Transonic Small-Disturbance Equation," *Journal of Aircraft*, Vol. 25, No. 7, 1988, pp. 598–605.

[30]Flake, R. H., "Volterra Series Representation of Nonlinear Systems," Pt. II: Applications and Industry, *Transactions of the American Institute of Electrical Engineers*, Vol. 81, 1962.

[31]Ibrahim, R. A., "Response Analysis of Nonlinear Systems Using Functional-Perturbational Type Approach," 6th International Modal Analysis Conf., Union College and Society for Experimental Mechanics, Kissimmee, FL, Feb. 1–4, 1988, pp. 1480–1488.

[32]Batina, J. T., Seidel, D. A., Bland, S. R., and Bennett, R. M., "Unsteady Transonic Flow Calculations for Realistic Aircraft Configurations," *Journal of Aircraft*, Vol. 26, No. 1, 1989, pp. 21–28.

[33]Bennett, R. M., Bland, S. R., Batina, J. T., Gibbons, M. D., and Mabey, D. G., "Calculation of Steady and Unsteady Pressures on Wings at Supersonic Speeds with a Transonic Small-Disturbance Code," AIAA/ASME/ASCE/AHS 28th Structures, Structural Dynamics, and Materials Conf., AIAA Paper 87-0851, Monterey, CA, April 6–8, 1987.

[34]Batina, J. T., "Unsteady Transonic Algorithm Improvements for Realistic Aircraft Applications," *Journal of Aircraft*, Vol. 26, No. 2, 1989, pp. 131–139.

[35]Batina, J. T., "Unsteady Transonic Small-Disturbance Theory Including Entropy and Vorticity Effects," *Journal of Aircraft*, Vol. 26, No. 6, 1989, pp. 531–538.

[36]Silva, W. A., and Bennett, R. M., "Predicting the Aeroelastic Behavior of a Wind-Tunnel Model Using Transonic Small Disturbance Theory," Seventeenth Congress of the International Council of the Aeronautical Sciences, Stockholm, Sweden, Sept. 9–14, 1990, pp. 1–10.